HHS Public Access

Author manuscript

Biomacromolecules. Author manuscript; available in PMC 2016 February 09.

Published in final edited form as:

Biomacromolecules. 2016 February 8; 17(2): 399–406. doi:10.1021/acs.biomac.5b01168.

Thermoresponsive and Mechanical Properties of Poly(L-proline) Gels

Manos Gkikas[†,#], **Reginald K. Avery**[‡,#], and **Bradley D. Olsen**[†,*]

[†]Department of Chemical Engineering, Massachusetts Institute of Technology, Cambridge, Massachusetts 02139, United States

[‡]Department of Biological Engineering, Massachusetts Institute of Technology, Cambridge, Massachusetts 02139, United States

Abstract

Gelation of the left helical N-substituted homopolypeptide poly(L-proline) (PLP) in water was explored, employing rheological and small-angle scattering studies at different temperatures and concentrations in order to investigate the network structure and its mechanical properties. Stiff gels were obtained at 10 wt % or higher at 5 °C, the first time gelation has been observed for homopolypeptides. The secondary structure and helical rigidity of PLP has large structural similarities to gelatin but as gels the two materials show contrasting trends with temperature. With increasing temperature in D_2O, the network stiffens, with broad scattering features of similar correlation length for all concentrations and molar masses of PLP. A thermoresponsive transition was also achieved between 5 and 35 °C, with moduli at 35 °C higher than gelatin at 5 °C. The brittle gels could tolerate strains of 1% before yielding with a frequency-independent modulus over the observed range, similar to natural proline-rich proteins, suggesting the potential for thermoresponsive or biomaterial-based applications.

Graphical abstract

[*]**Corresponding Author**. bdolsen@mit.edu.

[#]M.G. and R.K.A. contributed equally.

ASSOCIATED CONTENT

Supporting Information

The Supporting Information is available free of charge on the ACS Publications website at DOI: 10.1021/acs.biomac.5b01168.

^{1}H NMR and FTIR of LP-NCA; GPC of PLP70 in 0.1 M $NaNO_3$ solution of water/acetonitrile 80:20 v/v; FTIR spectra of PLP in the solid state after synthesis and PLP II; Frequency and strain sweeps of PLP70 at 10 and 15 wt % at 5 and 35 °C; Frequency sweeps comparison of 10 wt % PLP70 at 35 °C with 10 wt % gelatin at 5 °C; Concentration dependence of modulus for PLP70 gels; SANS plots of PLP40 at 5 wt % at 5 and 35 °C; and table with all fitted values from model fitting (PDF).

The authors declare no competing financial interest.

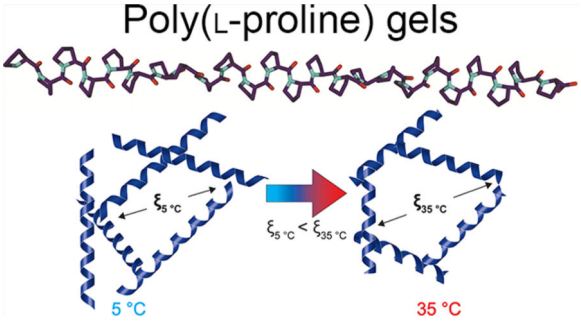

INTRODUCTION

Engineering the morphological and rheological properties of materials is of paramount importance, especially when different architectures and secondary structures are combined. Hydrogels as drug delivery scaffolds and tissue engineering tools have traditionally been constructed with hydrophilic polymers of high molecular weight, cross-linked through either covalent bonds or physically associating groups.[1–10] One example of these materials is synthetic polypeptides prepared by N-carboxy anhydride (NCA) polymerization,[11] yielding low dispersity, high molecular weight polypeptides,[12] which has led to hierarchical self-assembled nanoscale structures with tunable properties[13] and a wide range of biological applications.[14,15]

Most polypeptides of α-amino acids form 3D structures through hydrogen bonding. The exception is N-substituted polypeptides,[16–19] which do not possess an amide (3-N) hydrogen for the formation of hydrogen bonds. Their secondary structure is due only to the constraints imposed by the main chain. The lone natural N-substituted polypeptide is poly(L-proline) (PLP),[18] which is the only pH-independent, aliphatic, water-soluble, helical polypeptide.[17] It is characterized by hydrophilic interactions (hydrogen bond donation by water molecules to both the tertiary amine and the carbonyl group) and hydrophobic interactions (pyrrolidine rings). Due to PLP's rigid backbone, containing consecutive pyrrolidine rings and resonance-stabilized imide peptide linkages, it can serve as a scaffold for protein–protein recognition, molecular identification, enzyme tetramerization, and cell penetration,[20] while the large effect of the polyproline helix on the protein conformation renders PLP a useful model for the study of native proteins such as gelatin and collagen.[21]

PLP contains tertiary amide groups which significantly lower the barrier for *cis–trans* amide isomerization[22] and result in two conformations: PLP I, a compact right-handed helix, where the peptide bonds adopt the *cis* conformation, and PLP II, a stretched left-handed helix where the peptide bonds adopt the *trans* conformation. PLP I has an axial translation of 1.9 Å (3.3 residues/turn) and is favored in aliphatic alcohols.[23] PLP II is a highly extended polypeptide structure with a 3.1 Å axial translation (3 residues/turn) and is favored in water and organic acids[17,22] due to simultaneous hydrogen bond donation to both the carbonyl group and the tertiary amine. Since the peptide groups control the final conformation and are accessible to the solvent, the PLP I to PLP II transition depends on the solvent composition, ionic strength and acidity.[22,24] While *cis*-proline residues are postulated to account for certain conformational features in proteins, *trans*-proline residues (PLP II) commonly occur

in globular proteins and are often found in turns or at the edge strands of antiparallel β-sheets, disrupting the ordered conformation.[5a,25]

Polymerization in organic solvents favors the PLP I form of the helix, which has low solubility in water.[17] Dissolution in water, catalyzed either by organic acids or incubation at low temperature (between −15 and 5 °C),[26] leads to mutarotation of the helix into the PLP II form. Alternatively, increasing the temperature to around 63–65 °C precipitates dilute PLP II aqueous solutions and upon cooling, the helices can be redissolved.[26] Light scattering, X-ray diffraction (XRD), and turbidity studies have indicated that PLP's phase change involves crystallization from solution with increasing temperature, similar to the thermal precipitation of tropocollagen.[26] Heating leads to aggregation[27,28] or a PLP II to PLP I transition,[26] due to the disruption of hydrogen bonding. Kinetic effects and differing XRD patterns for the precipitates have resulted in a discord in the type of transition, either a liquid to crystal,[26] or a liquid to liquid first-order transition.[27] The transition temperature depends on the rate of heating, with higher transition temperatures observed for faster heating rates.[27] The observation of thermoresponsive properties in dilute solutions suggests that more concentrated PLP solutions may be able to exhibit thermoresponsive gelation behavior with consequent changes in mechanical properties.

Herein, the gelation behavior of concentrated aqueous PLP solutions in water is explored, employing rheological and small-angle neutron scattering (SANS) studies at different temperatures and concentrations in order to investigate the network structure and its relative homogeneity. Stiff gels were obtained at 10 wt % or higher at 5 °C, the first-time gelation has been observed for homopolypeptides. Temperature-dependent mechanical properties and structural changes were examined in the material when temperature was increased from 5 to 35 °C, providing insight into the effect of temperature on PLP gelation.

EXPERIMENTAL METHODS

Materials

Boc-L-proline-OH (Boc-Pro-OH, >99%), triphosgene (99%), triethylamine (>99%), and hexylamine (>99%) were purchased from Aldrich. Amine-free acetonitrile was purchased from Fisher. D_2O was purchased from Cambridge Isotopes.

Synthesis of L-Proline N-Carboxy Anhydride (LP-NCA)

The monomer was synthesized according to established procedures.[18a] *tert*-Butyloxycarbonyl-L-proline (14 g, 0.065 mol) was dissolved in dry THF (600 mL) in a 1 L, two-necked, round-bottom flask, with a slight flow of dry N_2. Then, triphosgene (7.1 g, 0.024 mol) was added under vigorous stirring. After 10 min, triethylamine (7.2 g, 0.072 mol) was added dropwise at 0 °C, leading to the formation of N-carboxy anhydride in a one-pot procedure with instantaneous precipitation of TEA·HCl salt. After stirring for 6.5 h at room temperature under a N_2 atmosphere, the precipitate was removed by filtration. The filtrate was then rotovapped, and the crude mixture was dissolved in ethyl acetate, chilled, and extracted with ice-cold water until neutral pH was reached. The organic phase was then separated, dried with $(Na)_2SO_4$, and the solvent was rotovapped, yielding 8 g of crude LP-

NCA. The crude LP-NCA was dissolved in the minimum amount of THF (~30 mL), and a large excess of hexane (400 mL) was added, leading to a white, thick precipitate that was cooled to −20 °C for complete precipitation. The solvent mixture was then decanted under a dry N_2 flow, and the LPNCA crystals were dried under vacuum, resulting in a final purified yield of 4.5–5 g (50%). The procedure was repeated two more times and the final product was characterized by ^{1}H NMR and FTIR (Figures S1 and S2). The pure product was then stored in the glovebox.

LP-NCA. ^{1}H NMR (500 MHz, $CDCl_3$) δ 4.34 (dd, J = 8.78, 7.84 Hz, 1H), 3.78 (dt, J = 11.4, 7.47, 7.47 Hz, 1H), 3.34 (ddd, J = 11.4, 8.32, 4.92 Hz, 1H), 2.45−2.05 (m, 3H), 1.95 (m, 1H); FTIR (deposited on KBr cards) 2996, 2957, 1845, 1824, 1772, 1368, 1332, 1274, 1207, 1188, 1155, 1100, 1019, 1006, 955, 922 cm^{-1}.

Synthesis of Poly(L-prolines) (PLPs)

The desired amount of LPNCA (2.5 g, 0.018 mol) was added in a dry, air-free, Schlenk flask inside a glovebox, immediately transferred to the nitrogen/vacuum line, and purged with a continuous nitrogen flow. The monomer was then dissolved in amine-free acetonitrile (~15 mL), and hexylamine was added. After addition of the hexylamine (2.5 g, 0.22 × 10^{-3} mol, NCA/initiator = 82 for PLP70), the solution became opaque. After stirring for 1 week under N_2, a milky solution was obtained. At the end of the reaction, the polymer was precipitated in cold ether, filtered, and dried in vacuum. The resulting polymer contained both helical forms (mainly form I), as quantified by solid-state FTIR. In order to obtain the fully water-soluble PLP II, the polypeptide was suspended in ultrapure (Milli-Q) water and stirred for 1–2 days at 4 °C, changing from a milky solution to a clear aqueous solution. The polymer was filtered, dialyzed extensively against Milli-Q water, and lyophilized to give a final purified yield of 1.3 g PLP II (75%), in agreement with previous studies.

PLP II. ^{1}H NMR (500 MHz, CF_3COOD) δ 4.92 (1H, C^{α}), 3.95−3.75 (2H, C^{δ}), 2.46−2.15 (4H, $C^{\beta+\gamma}$); GPC (5% NaH_2PO_4) water/ACN 97:3 at 35 °C, M_w/M_n = 1.28–1.32; FTIR (deposited on KBr cards) 3450, 2962, 2879, 1640, 1448, 1431, 1351, 1333, 1315, 1261, 1206, 1164, 1094, 1040, 916 cm^{-1}.

The molecular weight of PLP II was calculated by GPC and ^{1}H NMR. Due to the fact that the polydispersity is higher than living polymerization due to heterogeneous polymerization, the degree of polymerization was estimated by end-group analysis by ^{1}H NMR. The molecular weight was calculated by comparing the C^{α} proton (4.92 ppm, 1H) to the hexylamine protons (0.84 ppm, 3H), as is shown in Figure 1. Depending on the LP-NCA/hexylamine molar feed, different molecular weights of PLP II were obtained (Table 1). GPC in water/acetonitrile (80/20 v/v) as well as FTIR characterization in the solid state were also recorded (Figures S3 and S4).

Gelation

Lyophilized PLP II samples were weighed into Eppendorf tubes and Milli-Q water (for rheology, CD studies) or D_2O (for SANS studies) was added to achieve the desired concentration. The milky samples obtained were thoroughly mixed by vortexing and were

stored at −20 °C for 5 min. After removal from −20 °C and thawing at room temperature, the PLP samples became transparent, viscous solutions or gels, depending on concentration. Samples were stored at 4 °C until testing. The incubation and storage temperatures were found to be critical since, at higher temperatures, the stability of the samples was impacted, leading to blurry solutions.

Characterization Methods

FTIR measurements were performed with a Thermo Nicolet Nexus 870 instrument. Solutions were deposited on KBr real crystal IR cards. The spectra were collected over the range 450–3800 cm^{-1} and corrected for KBr background. ^{1}H NMR spectroscopy (500 MHz) was performed using a Varian Inova 502 spectrometer. The spectra of the polymers were acquired in CF_3COOD, and the spectrum of L-proline NCA (LP-NCA) was taken in $CDCl_3$. GPC analysis (Waters Breeze 2410) was performed at 5 mg/mL in a 0.1 M $NaNO_3$ solution of water/acetonitrile (80/20 v/v) at a flow rate of 0.8 mL/min at 35 °C using PEO standards. CD measurements were performed with an Aviv Model 202 Circular Dichroism spectrometer in a 0.1 cm path length cuvette to measure far UV circular dichroism spectroscopy over the range 183–240 nm. Measurements were performed at 1 mg/mL, with a scan rate of 12 nm/min.

Rheology Measurements

Rheology was performed on an Anton-Paar 702 rheometer using the single drive configuration. A sandblasted 25 mm diameter cone with a 1° angle (CP25−1/S geometry) and a Peltier-controlled bottom plate were used for all measurements to avoid slip at the sample–tool interface. Samples were loaded at 5 °C, sealed with mineral oil to prevent evaporation, and allowed to equilibrate for 1 h. Samples were then heated to 35 °C, equilibrated for an hour, cooled to 5 °C, and equilibrated for one more hour before measurement. Strain sweeps were performed at 5 and 35 °C at 1 rad/s from 0.1 to 10% strain to determine the linear viscoelastic region (Figures S5). Frequency sweeps were acquired from 0.01 to 100 rad/s at 5 and 35 °C at 0.1% strain. Thermal cycles were performed, alternating between 3 h periods at 5 and 35 °C, at 0.1% strain and 1 rad/s. After temperature cycling, frequency sweeps were run at 5 and 35 °C over the range 0.01–100 rad/s at 0.1% strain, within the linear regime at all frequencies.

SANS Measurements

Samples were studied on the Bio-SANS beamline at the High Flux Isotope Reactor (HFIR) at Oak Ridge National Laboratory and measured over the q-range of 0.003–0.4 $Å^{-1}$. All 1 wt % samples were loaded into 1 mm path length quartz banjo cells, while higher concentration PLP samples were loaded into brass sample holders, containing a Teflon spacer with a 10 mm diameter hole sandwiched between two quartz disc windows. All samples were measured at 5 and 35 °C, with a 6 Å neutron wavelength. One hour equilibrations were allowed at each temperature before sample data was collected. A sample aperture of 10 mm was used for banjo cells, and a 6 mm aperture was used for brass holders. The scattering data was reduced using the SPICE SANS reduction package and corrected for D_2O background at 5 and 35 °C. Data was then fit to a modified correlation length model, the

original model developed by Hammouda and co-workers,[29,30] through a nonlinear, least-squares fit using the curve fitting tool in Igor Pro. This model has been used to analyze the scattering spectra of polymer solutions as well as scattering from hydrogel systems. The scattering intensity is modeled by the following equation:

$$I(q)=\frac{A}{q^n}\times\frac{C}{1+(|q-q_0|\xi)^m}+\frac{B}{q^p}$$

where $I(q)$ is the scattering intensity, q is the scattering vector, q_0 is related to the broad peak location, and B is scattering from background. Parameters n, m, and ξ are the Porod exponent, the Lorentzian exponent, and the Lorentzian screening length, respectively. The Porod exponent, n, characterizes the fractal structure of the gel, while the Lorentzian exponent, m, characterizes the polymer–solvent interactions, describing the system's thermodynamics.[29,30] The exponent, p, provides a minor correction that improves fitting at higher q values, especially for scattering curves of low temperature and concentration, where a plateau in the intensity is not present. The Lorentzian screening length, ξ, is the correlation length for polymer chains and, in the case of gel networks, it gives an indication of the gel mesh size.

RESULTS AND DISCUSSION

Gelation of PLP

Unlike most homopolypeptide solutions, PLP formed gels at sufficiently high concentrations. The helical homopolypeptide PLP gelled at 5 °C at 10 wt % or above. Figure 2a shows frequency sweeps of 1, 10, and 15 wt % PLP70 samples at 5 °C. Though PLP70 at 1 wt % also has a value of G' exceeding G'', it failed the simple inversion test which is passed for 10 wt % or above. For a viscoelastic fluid with this low of a modulus, the yield stress can be overcome by gravity, exhibiting effectively liquid-like behavior. The storage modulus increased with increasing concentration and was independent of frequency for both 10 and 15 wt % samples within the measured range. This is the first observation of gelation for homopolypeptides (Figure 2b). Scattering results for the PLP70 samples showed a qualitative change in scattering pattern as the concentration was increased from dilute solution into the gelation regime (Figure 2c). In the low concentration regime (1 wt % PLP70), the scattering pattern showed a power law type decay with only a very weak shoulder. No Guinier regime was observed even for $qL_{PLP} \ll 1$, indicative of strong intermolecular associations even at these low concentrations. The data was fitted by the modified correlation length model, originally developed by Hammouda.[29,30] In 1 wt % PLP70, the power decay at low q was 2.3. At this low concentration, a shoulder, due to the presence of a characteristic length within the system was weak and the correlation length was approximately 4.4 nm. The upturn seen at low q is characteristic for semidilute solutions of water-soluble polymers.[29,30]

At high concentrations, the effect of intermolecular correlations and large scale concentration fluctuations became more pronounced, as indicated by the appearance of a pronounced shoulder and a large increase in the low q scattering intensity. Fitting with the

modified correlation length model showed a slight increase in correlation length with increasing concentration. For 10 and 15 wt % PLP70 at 5 °C, ξ was calculated to be 5.0 and 5.5 nm, respectively (Tables 2 and S1), a typical value for concentrated polymer solutions or hydrogels,[2–4,29,30] while the expected helix length for PLP II is R_0 = 21.7 nm (assuming a fully extended helix with 3.1 Å/residue for 70 units). This suggested that the chain correlations were occurring on the submolecular length scale. The power law at low q for both 10 and 15 wt % PLP70 at 5 °C was calculated to be 2.5, slightly higher than the low concentration regime. In both the low and high concentration regime, the low q power law was consistent with a mass fractal with a dimensionality of approximately 2.5.

Heating of dilute PLP solutions to elevated temperatures has been reported to lead to a highly packed state.[28] Analogous to thermoresponsive precipitation from solution, heating PLP gels resulted in responsive changes in their structural (Figure 3a) and mechanical properties (Figure 3b,c). A shift to higher wavelengths in the characteristic negative peak of the polyproline II helix is observed in circular dichroism (CD) upon heating dilute PLP solutions, accompanied by a decrease in the intensity of the peak. The red-shift observed in the characteristic strong negative band from 201 nm at 0 °C to 203 nm at 35 °C is shown in Figure 3a. The decreasing intensity of the CD peak with increasing temperature is characteristic of a decrease in the helicity of the PLP II helix.[31] It has been suggested that the above spectral changes arise from a greater chain rigidity at lower temperatures, which give rise to an effectively longer spectroscopic unit,[31] since the extended PLP II structure is favored in water or at low temperatures.[22,26] Furthermore, it has been calculated that the binding of water to the imide groups tends to rigidify the chain.[32] Heating of a PLP II dilute solution leads to a weakening interaction between the chain and the bound water, with PLP II ultimately precipitating as a crystalline solid at high enough temperatures.[26] At the same time, elevated temperatures also contributed to enhanced chain motion and flexibility. Thus, the data reflects a loosening of the 3_1 structure of PLP II as the temperature is raised, leading to a decrease in the magnitude and a red-shift of the negative peak in the CD spectrum. The change in CD with temperature is not very large but implies a decrease in the helicity in dilute solutions, typical for PLP.[31] Since there was no clear PLP II to PLP I transition, an intermediate structure is assumed to be present during the increase in temperature, which is expected to lead to lower actual dimensions.[24c]

The partial disruption of hydrogen bonding in the PLP helix upon heating leads to increased intermolecular aggregation at higher temperatures, resulting in changes in gel mechanical properties. Equilibrated gels were cycled between 3 h periods at 35 and 5 °C while monitoring the modulus, highlighting the thermoresponsive nature of the gels. Cycles were reproducible and consistent after the first measurement for 10 wt % PLP70 at 5 °C (Figure 3b), exhibiting limit cycle behavior starting from the second cycle. No thermal cycle or long relaxation time was able to recover the initial modulus of the gel, suggesting strong kinetic effects on the structure due to the presence of associative interactions under all accessible experimental conditions. It was observed that, for PLP70, the moduli could evolve for up to 3 h after the initial step change in temperature, indicating slow dynamics of structural rearrangement that are consistent with an influence of kinetic effects on the gel modulus and the inability to reverse the effects of thermal history. The storage moduli values obtained for

PLP70 at 35 °C were higher than or comparable to those reported for gelatin (Figure S6), collagen-mimetic peptides,[7] Matrigel,[34] RADA16,[33] and β-sheet formed hydrogels.[5,34,35]

Frequency sweeps at both 5 and 35 °C showed no dependence of moduli on frequency between 0.01 and 100 rad/s (Figure S7). This suggests very slow relaxation times in highly concentrated PLP systems and implies that the physically cross-linked structure is not dynamic on the time scale of the experiment. There is an increased dependence of the modulus on the concentration after heating the samples to 35 °C (Figure 4a) when compared to the plateau moduli observed at 5 °C, which leads to an order of magnitude higher moduli for 35 °C, 15 wt % PLP70 (~10^5 Pa) than 35 °C PLP70 at 10 wt % (~10^4 Pa). The observed frequency independence of PLP is also seen in gelatin (Figure S6), collagen,[33,36] and collagen-mimetic peptides,[7] all having a high-proline content and suggesting a correlation with the secondary structure of the polyproline helix. However, the dependence of moduli on temperature for the PLP gels was opposite that of gelatin gels (Figure S6): when the gelatin/collagen gels are heated they undergo a sol–gel transition to a liquid state, while the PLP gels undergo a gel stiffening transition over the same temperature range. While in both cases heating disrupts hydrogen bonding, the gelatin sequence contains many charged and polar residues that contribute to high temperature solubility, while the PLP helix does not. Therefore, at high temperature, the PLP helix rearranges into an aggregated state. Due to these properties and their local rigidity, proline-rich sequences have been considered as favorable sites for nucleation in gelatin gels.[37]

Scattering results for all the PLP70 samples showed increased low q scattering intensity at 35 °C. This feature became more pronounced in 10 and 15 wt % gels (Figure 4b,c) at 35 °C as the weight fraction of PLP was increased, suggesting that heating the samples resulted in an increase in the magnitude of concentration fluctuations at larger length scales within the sample. By fitting the data to the modified correlation length model (Tables 2 and S1), small increases in the correlation length were detected after heating at the same concentration. For the 10 wt % PLP70, ξ was calculated to be 6.7 nm at 35 °C, while for 15 wt % PLP70, ξ was calculated as 7.2 nm. The power law of the low q regime decreased slightly with heating for both concentrations. However, the measured value of 2.2 for the power decay in both 10 and 15 wt % PLP70 at 35 °C continues to be consistent with a mass fractal structure.

Higher hydrogel moduli and increased scattering were obtained with increasing molar mass. A comparative study of 10 wt % gels for PLP50 and PLP70 at 5 °C is shown in Figure 5, where frequency sweeps of PLP50 and PLP70 are plotted (Figure 5a). Higher modulus was seen at 5 °C for the PLP70 sample in comparison with PLP50. Scattering results obtained (Figure 5b) also reveal higher scattering intensity for PLP70 at 5 °C, with a broad feature at q_{max} = 0.0223 Å−1. Structural differences were observed at elevated temperature (35 °C) at both molar masses (Figure 5c,d). Frequency sweeps of PLP50 and PLP70 at 10 wt % showed independence of moduli on frequency at 35 °C, as well as higher moduli for both samples (Figure 5a,c). PLP50 showed a broad shoulder at q_{max} = 0.0234 Å−1 (Figure 5d), which is consistent with lower molecular weights (Figure S8). By fitting the data to the modified correlation length model (Tables 2 and S1), a decrease in the mesh size was inferred with increasing molecular weight. For 10 wt % PLP50, ξ was calculated to be 5.5 nm at 5 °C (the expected length for a fully stretched PLP50 in form II is R_0 = 15.5 nm),

while for 10 wt % PLP70 the obtained value was 5.0 nm. By heating to 35 °C, the obtained ξ value was 10.2 nm for PLP50 and 6.7 nm for PLP70. The power law of the low *q* regime at 5 °C was higher for PLP50 than for PLP70, with a measured Porod exponent of 3.2 for PLP50 and 2.5 for PLP70. The same trend persisted at 35 °C, with values of 2.8 and 2.2 obtained for PLP50 and PLP70, respectively.

Structural information from SANS suggests that PLP forms gels due to aggregation of helices into a random network. The gels were clear at 5 °C, implying that there is no macrophase separation. Gelation occurs at a relatively high concentration of about 10 wt %, and the scattering model is consistent with a random network. By comparing the expected dimensions of an ideal fully extended PLP II chain (Table 1) with the correlation length value (mesh size) found in PLP gels (Tables 2 and S1), the mesh size is observed to be smaller than the theoretical length calculated from the pitch of PLP II (15.5 nm for ideal PLP50 vs 5.5 nm in 10 wt % PLP50; 21.7 nm for ideal PLP70 vs 5.0 nm in 10 wt % PLP70 at 5 °C). This is consistent with multiple intersections within the same chain in a randomly interconneted network, as illustrated in Figure 6. Both increasing temperature and increasing concentration lead to increased aggregation of the polymer chains. Under these conditions, SANS shows both higher low *q* scattering intensity and a slightly larger mesh size in the gels. This suggests that increased aggregation yields larger concentration fluctuations between PLP-rich and PLP-poor regions and, consequently, the formation of a moderately larger mesh size. The higher degree of aggregation at higher concentration or higher temperature (increased interchain interactions due to partial helix unfolding) are both also manifest in the observed thermoresponsive stiffening transition.

There is also a substantial effect of molar mass on the gel properties even for a small change in chain length. Increasing chains from 50 to 70 repeat units results in a large increase in modulus, presumably due to the increased number of interactions per chain and consequently increased percolation of the network. While at 10 wt % at 5 °C the two networks have a similar mesh size, heating results in a more substantial increase in mesh size for PLP50 than for PLP70. Because the decreased number of interactions per chain should make PLP50 chains somewhat less kinetically hindered, it is hypothesized that the larger change in mesh size for shorter chains results from the fact that they are more kinetically mobile to rearrange in response to increased intramolecular interactions at high temperautre.

CONCLUSIONS

The linear rheology of highly concentrated aqueous poly(L-proline) solutions was examined, showing gelation at 5 °C and 10 wt % concentrations or above, the first observation of a gel in homopolypeptides prepared by the ring-opening polymerization of NCAs. The elastic modulus was independent of frequency between 0.01 and 100 rad/s, characteristic of gelatin, collagen, and collagen-mimetic peptides, revealing slow dynamics in the physically cross-linked network. Heating the samples to 35 °C revealed a thermoresponsive transition from a softer to a stiffer gel, having the opposite trend that is observed in gelatin gels. SANS studies showed a network transition in D_2O at 35 °C, with broad features corresponding to approximately the same correlation length for different molecular weights. The

thermoresponsive, frequency-independent, and stiff gel properties of concentrated PLP networks makes them a unique type of homopolypeptide system, with the ability to serve as model materials for understanding other proline-rich protein sequences or function as new thermoresponsive and biocompatible materials.

Supplementary Material

Refer to Web version on PubMed Central for supplementary material.

Acknowledgments

This work was supported by the U.S. Army Research Office under contract W911NF-13-D-0001. We thank ORNL for support in the SANS experiments and especially Urban Volker for his guidance, as well as Boualem Hammouda for helpful discussions. We also acknowledge the MIT Department of Chemistry Instrumentation Facility for the NMR instrumentation and the Biophysical Instrumentation Facility for the CD spectroscopy work. R.K.A. was supported by an NIH Interdepartmental Biotechnology Training Program (NIH/NIGMS 5T32GM008334)

REFERENCES

1. Kim M, Tang S, Olsen BD. J. Polym. Sci., Part B: Polym. Phys. 2013; 51:587–601.
2. Matsunaga T, Sakai T, Akagi Y, Chung UI, Shibayama M. Macromolecules. 2009; 42:6245–6252.
3. Saffer EM, Lackey MA, Griffin DM, Kishore S, Tew GN, Bhatia SR. Soft Matter. 2014; 10:1905–1916. [PubMed: 24652367]
4. (a) Pochan DJ, Pakstis L, Ozbas B, Nowak AP, Deming TJ. Macromolecules. 2002; 35:5358–5360. (b) Nowak AP, Breedveld V, Pakstis L, Ozbas B, Pine DJ, Pochan D, Deming TJ. Nature. 2002; 417:424–428. [PubMed: 12024209]
5. (a) Schneider JP, Pochan DJ, Ozbas B, Rajagopal K, Pakstis L, Kretsinger J. J. Am. Chem. Soc. 2002; 124:15030–15037. [PubMed: 12475347] (b) Breedveld V, Nowak AP, Sato J, Deming TJ, Pine DV. Macromolecules. 2004; 37:3943–3953.
6. (a) Nichol JW, Koshy ST, Bae H, Hwang CM, Yamanlar S, Khademhosseini A. Biomaterials. 2010; 31:5536–5544. [PubMed: 20417964] (b) Gandhi SS, Yan H, Kim C. ACS Macro Lett. 2014; 3:1210–1214.
7. O'Leary LER, Fallas JA, Bakota EL, Kang MK, Hartgerink JD. Nat. Chem. 2011; 3:821–828. [PubMed: 21941256]
8. Gaharwar AK, Avery RK, Assmann A, Paul A, McKinley GH, Khademhosseini A, Olsen BD. ACS Nano. 2014; 8:9833–9842. [PubMed: 25221894]
9. Glassman MJ, Chan J, Olsen BD. Adv. Funct. Mater. 2013; 23:1182–1193. [PubMed: 25568642]
10. (a) Huang J, Hastings CL, Duffy GP, Kelly HM, Raeburn J, Adams DJ, Heise A. Biomacromolecules. 2013; 14:200–206. [PubMed: 23190093] (b) Yeon B, Park MH, Moon HJ, Kim S-J, Cheon YW, Jeong B. Biomacromolecules. 2013; 14:3256–3266. [PubMed: 23909492] (c) Liu D-L, Chang X, Dong C-M. Chem. Commun. 2013; 49:1229–1231.(d) Zhang S, Alvarez DJ, Sofroniew MW, Deming TJ. Biomacromolecules. 2015; 16:1331–1340. [PubMed: 25748800]
11. (a) Kricheldorf HR. Angew. Chem., Int. Ed. 2006; 45:5752–5784.(b) Deming TJ, Curtin SA. J. Am. Chem. Soc. 2000; 122:5710–5717.(c) Hernandez HR, Klok H-A. J. Polym. Sci., Part A: Polym. Chem. 2003; 41:1167–1187.(d) Dimitrov I, Schlaad H. Chem. Commun. 2003; 23:2944–2945.(e) Zhang Y, Lu H, Lin Y, Cheng J. Macromolecules. 2011; 44:6641–6644. [PubMed: 22049249] (f) Mavrogiorgis D, Bilalis P, Karatzas A, Skoulas D, Fotinogiannopoulou G, Iatrou H. Polym. Chem. 2014; 5:6256–6278.
12. (a) Hadjichristidis N, Iatrou H, Pitsikalis M, Sakellariou G. Chem. Rev. 2009; 109:5528–5578. [PubMed: 19691359] (b) Cheng J, Deming TJ. Top. Curr. Chem. 2011; 310:1–26. [PubMed: 21647839]
13. (a) Klok H-A, Lecommandoux S. Adv. Mater. 2001; 13:1217–1229.(b) Engler AC, Lee H-I, Hammond PT. Angew. Chem., Int. Ed. 2009; 48:9334–9338.(c) Chopko CM, Lowden EL, Engler

AC, Griffith LG, Hammond PJ. ACS Macro Lett. 2012; 1:727–731. [PubMed: 24883233] (d) Hamley I. Biomacromolecules. 2014; 15:1543–1559. [PubMed: 24720400]

14. (a) Osada K, Kataoka K. Adv. Polym. Sci. 2006; 202:113–153.(b) Deming TJ. WIREs Nanomed. Nanobiotechnol. 2014; 6:283–297.(c) Iatrou H, Dimas K, Gkikas M, Tsimblouli C, Sofianopoulou S. Macromol. Biosci. 2014; 14:1222–1238. [PubMed: 24838730]
15. (a) Meng F, Zhong Z, Feijen J. Biomacromolecules. 2009; 10:197–209. [PubMed: 19123775] (b) Schatz C, Louguet S, Le Meins J-F, Lecommandoux S. Angew. Chem., Int. Ed. 2009; 48:2572–2575.(c) Deng C, Wu J, Cheng R, Meng F, Klok H-A, Zhong Z. Prog. Polym. Sci. 2014; 39:330–364.
16. (a) Waley SG, Watson J. Proc. R. Soc. London, Ser. A. 1949; 199:499–517.(b) Cosani A, Palumbo M, Terbojevich M, Peggion E. Macromolecules. 1978; 11:1041–1045.
17. (a) Berger A, Kurtz J, Katchalski E. J. Am. Chem. Soc. 1954; 76:5552–5554.(b) Fasman GD, Blout ER. Biopolymers. 1963; 1:3–14.(c) Zhang A, Guo Y. Chem. Eur. J. 2008; 14:8939–8946. [PubMed: 18696526]
18. (a) Gkikas M, Iatrou H, Thomaidis NS, Alexandridis P, Hadjichristidis N. Biomacromolecules. 2011; 12:2396–2406. [PubMed: 21568310] (b) Graf R, Spiess HW, Floudas G, Butt H-J, Gkikas M, Iatrou H. Macromolecules. 2012; 45:9326–9332.(c) Gkikas M, Haataja JS, Ruokolainen, Iatrou H, Houbenov N. Biomacromolecules. 2015; 16:3686–3693. [PubMed: 26461162]
19. Gkikas M, Haataja JS, Seitsonen J, Ruokolainen, Ikkala O, Iatrou H, Houbenov N. Biomacromolecules. 2014; 15:3923–3930. [PubMed: 25260019]
20. (a) Sato S, Kwon Y, Kamisuki S, Srivastava N, Mao Q, Kawazoe Y, Uesugi M. J. Am. Chem. Soc. 2007; 129:873–880. [PubMed: 17243824] (b) Fillon YA, Anderson JP, Chmielewski J. J. Am. Chem. Soc. 2005; 127:11798–11803. [PubMed: 16104758] (c) Arora PS, Ansari AZ, Best TP, Ptashne M, Dervan PB. J. Am. Chem. Soc. 2002; 124:13067–13071. [PubMed: 12405833] (d) Crespo L, Sanclimens G, Montaner B, Perez-Tomas R, Royo M, Pons M, Albericio F, Giralt E. J. Am. Chem. Soc. 2002; 124:8876–8883. [PubMed: 12137542] (e) Biberoglu K, Schopfer LM, Tacal O, Lockridge O. FEBS J. 2012; 279:3844–3858. [PubMed: 22889087]
21. (a) Jenness DD, Sprecher C, Johnson WC Jr. Biopolymers. 1976; 15:513–521. [PubMed: 3232] (b) Shoulders MD, Raines RT. Annu. Rev. Biochem. 2009; 78:929–958. [PubMed: 19344236]
22. (a) Kurtz J, Berger A, Katchalski E. Nature. 1956; 178:1066–1067.(b) Gornick F, Mandelkern L, Diorio AF, Roberts DE. J. Am. Chem. Soc. 1964; 86:2549–2555.(c) Deber CM, Bovey FA, Carver JP, Blout ER. J. Am. Chem. Soc. 1970; 92:6191–6198. [PubMed: 5505620]
23. Steinberg IZ, Berger A, Katchalski E. Biochim. Biophys. Acta. 1958; 28:647–648. [PubMed: 13560425]
24. (a) Steinberg IZ, Harrington WF, Berger A, Sela M, Katchalski E. J. Am. Chem. Soc. 1960; 82:5263–5279.(b) Conti F, Piatelli M, Viglino P. Biopolymers. 1969; 7:411–415.(c) Shi L, Holliday AE, Shi H, Zhu F, Ewing MA, Russell DH, Clemmer DE. J. Am. Chem. Soc. 2014; 136:12702–12711. [PubMed: 25105554]
25. (a) Adzhubei A, Sternberg M. J. Mol. Biol. 1993; 229:472–493. [PubMed: 8429558] (b) Adzhubei A, Sternberg M, Makarov AA. J. Mol. Biol. 2013; 425:2100–2132. [PubMed: 23507311]
26. Ciferri A, Orofino TA. J. Phys. Chem. 1966; 70:3277–3285.
27. (a) Mandelkern L, Liberman L. J. Phys. Chem. 1967; 71:1163–1165. [PubMed: 6045205] (b) Engel J. Biopolymers. 1966; 4:945–948.
28. Tooke L, Duitch L, Measey TJ, Schweitzer-Stenner R. Biopolymers. 2010; 93:451–457. [PubMed: 19998404]
29. Hammouda B, Ho DL, Kline S. Macromolecules. 2004; 37:6932–6967.
30. Horkay F, Hammouda B. Colloid Polym. Sci. 2008; 286:611–620.
31. Tifany ML, Krimm S. Biopolymers. 1972; 11:2309–2316. [PubMed: 4634868]
32. Krimm S, Venkatachalam CM. Proc. Natl. Acad. Sci. U. S. A. 1971; 68:2468–2471. [PubMed: 5289879]
33. Mi K, Wang G, Liu Z, Feng Z, Huang B, Zhao XJ. Macromol. Biosci. 2009; 9:437–443. [PubMed: 19165822]

34. (a) Pochan DJ, Schneider JP, Kretsinger J, Ozbas B, Rajagopal K, Haines L. J. Am. Chem. Soc. 2003; 125:11802–11803. [PubMed: 14505386] (b) Ozbas B, Kretsinger J, Rajagopal K, Schneider JP, Pochan DJ. Macromolecules. 2004; 37:7331–7337.

35. Greenfield MA, Hoffman JR, Olvera de la Cruz M, Stupp SI. Langmuir. 2010; 26:3641–3647. [PubMed: 19817454]

36. Yang YL, Leone LM, Kaufman LJ. Biophys. J. 2009; 97:2051–2060. [PubMed: 19804737]

37. Djabourov M. Contemp. Phys. 1988; 29:273–297.

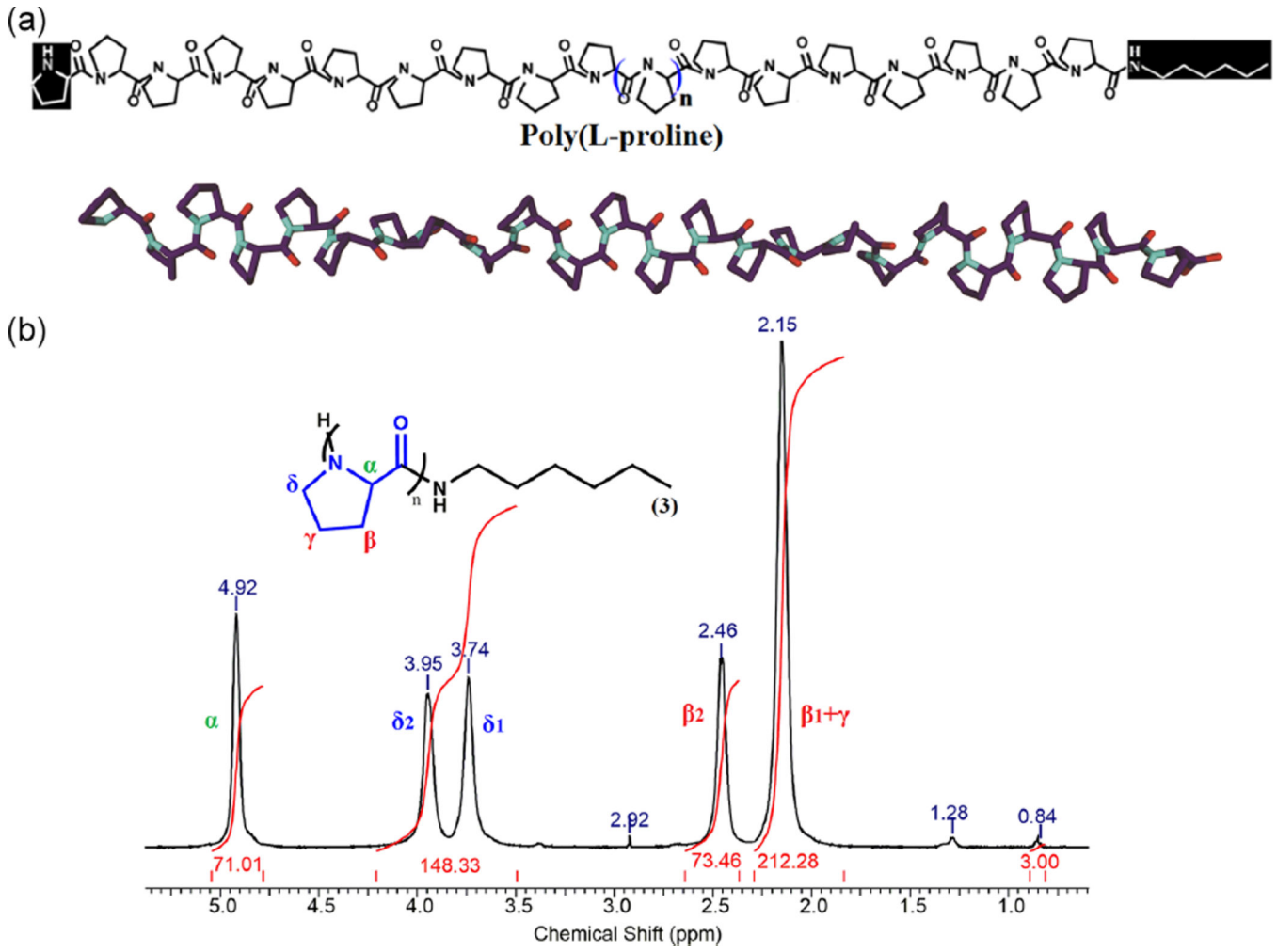

Figure 1.

(a) Chemical structure and stick structure of poly(L-proline) (PLP). The polypeptide cannot form internal hydrogen bonds, instead forming helices due to steric interactions between consecutive pyrrolidine rings. (b) ^{1}H NMR of PLP70 in CF_3COOD.

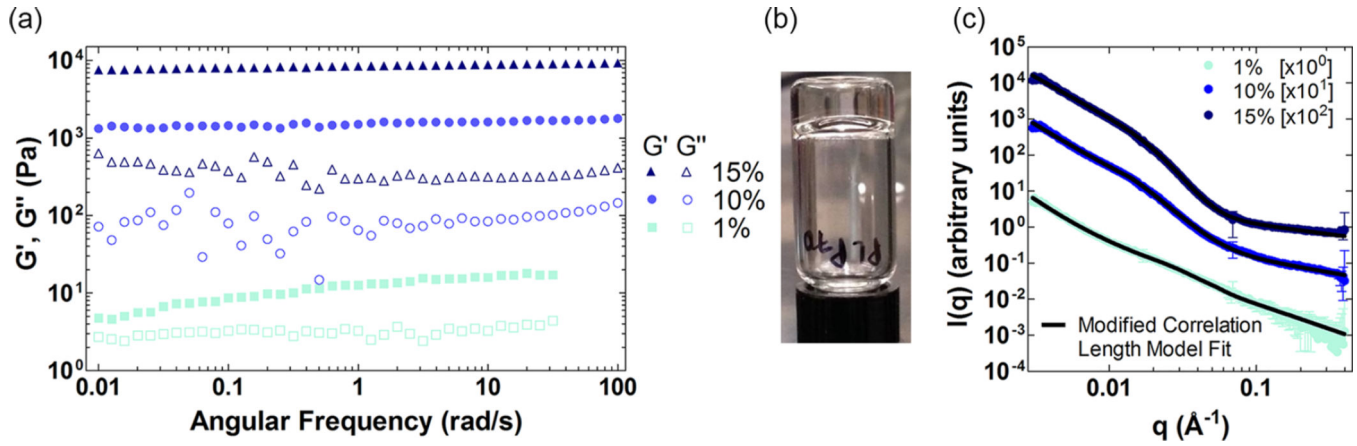

Figure 2.

(a) Frequency sweeps of 1, 10, and 15 wt % PLP70 at 5 °C at 0.1% strain. (b) Photo of PLP gel upon thawing at room temperature after 5 min at −20 °C. (c) SANS plots of 1, 10, and 15 wt % PLP70 in D_2O at 5 °C. SANS curves are offset for clarity.

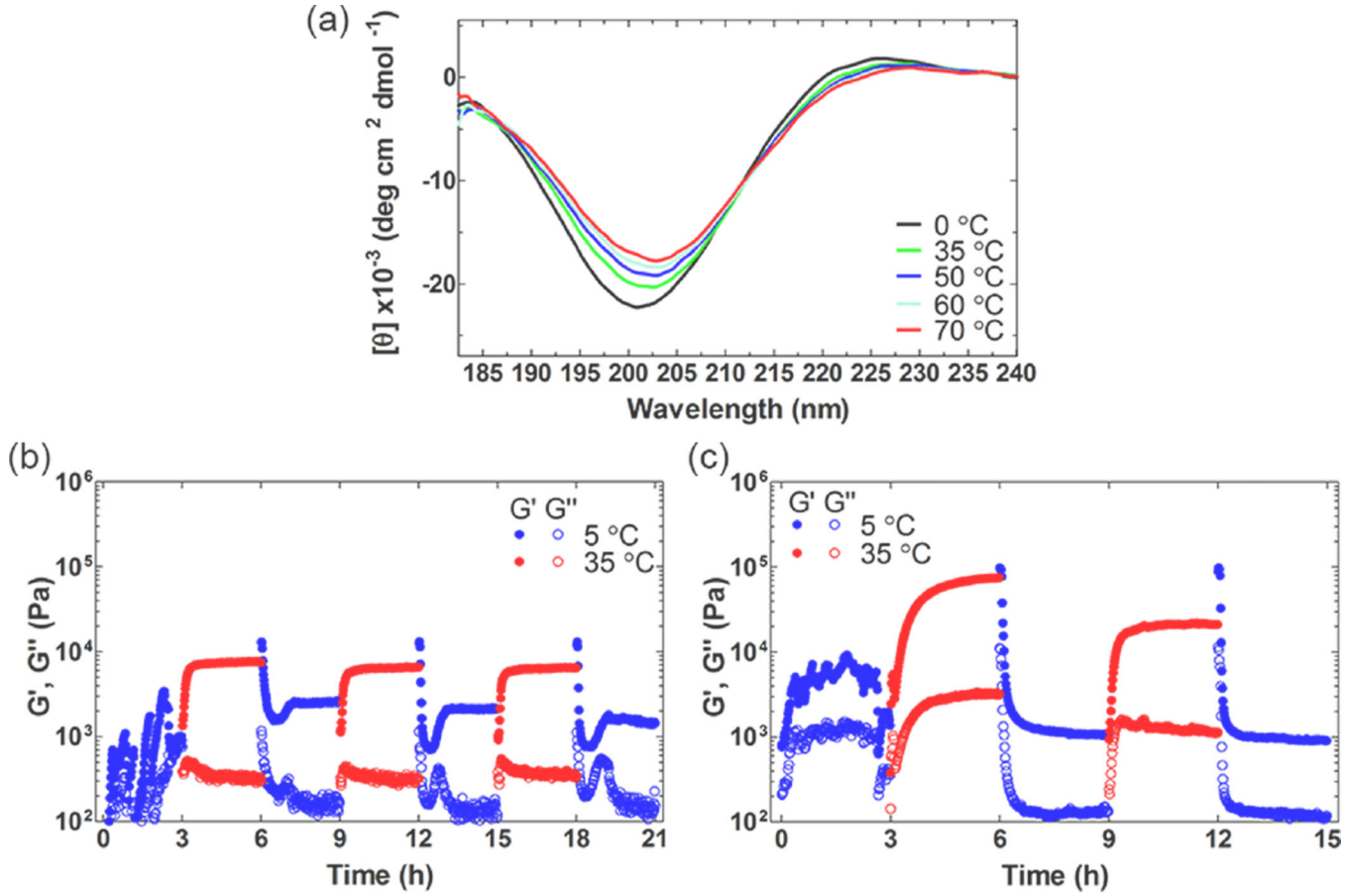

Figure 3.

(a) CD spectra of PLP70 in water, monitored from 0 to 70 °C, at 1 mg/mL. Temperature cycles were performed for (b) 10 wt % aqueous PLP70 and (c) 15 wt % aqueous PLP70. The thermal program involved rapid switching between 5 and 35 °C every 3 h while maintaining a 0.1% strain at an angular frequency of 1 rad/s.

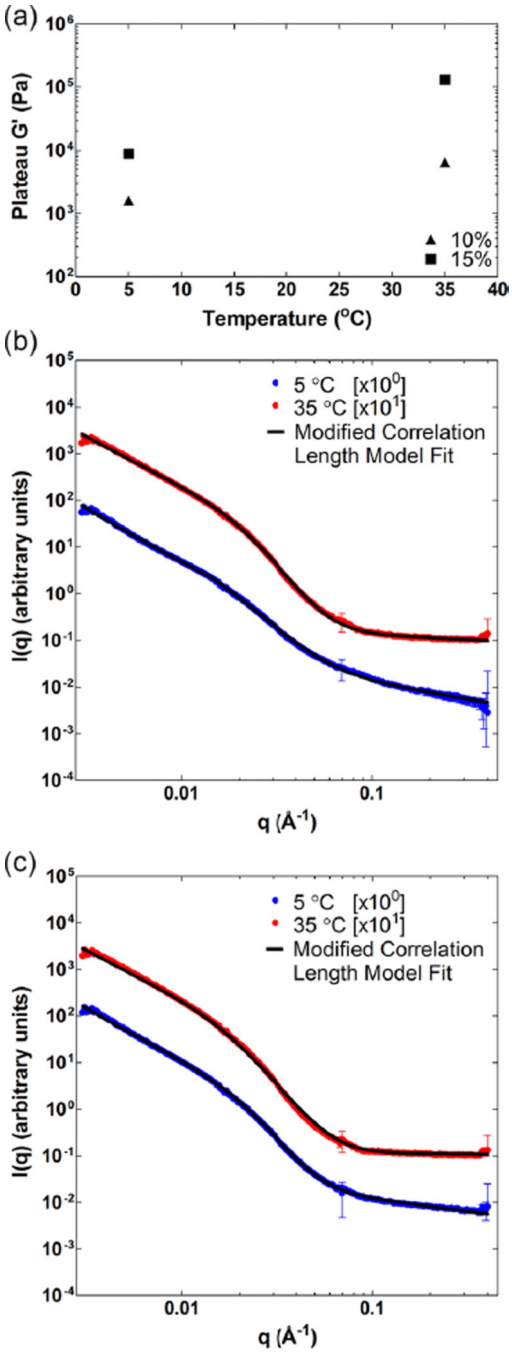

Figure 4.

(a) Dependence of the plateau modulus, measured at 10 rad/s, of 10 and 15 wt % PLP70 on temperature. SANS plots in D_2O for (b) 10 wt % PLP70 and (c) 15 wt % PLP70 at 5 and 35 °C. Gels were equilibrated at each temperature for 1 h prior to measurements. SANS curves are offset for clarity.

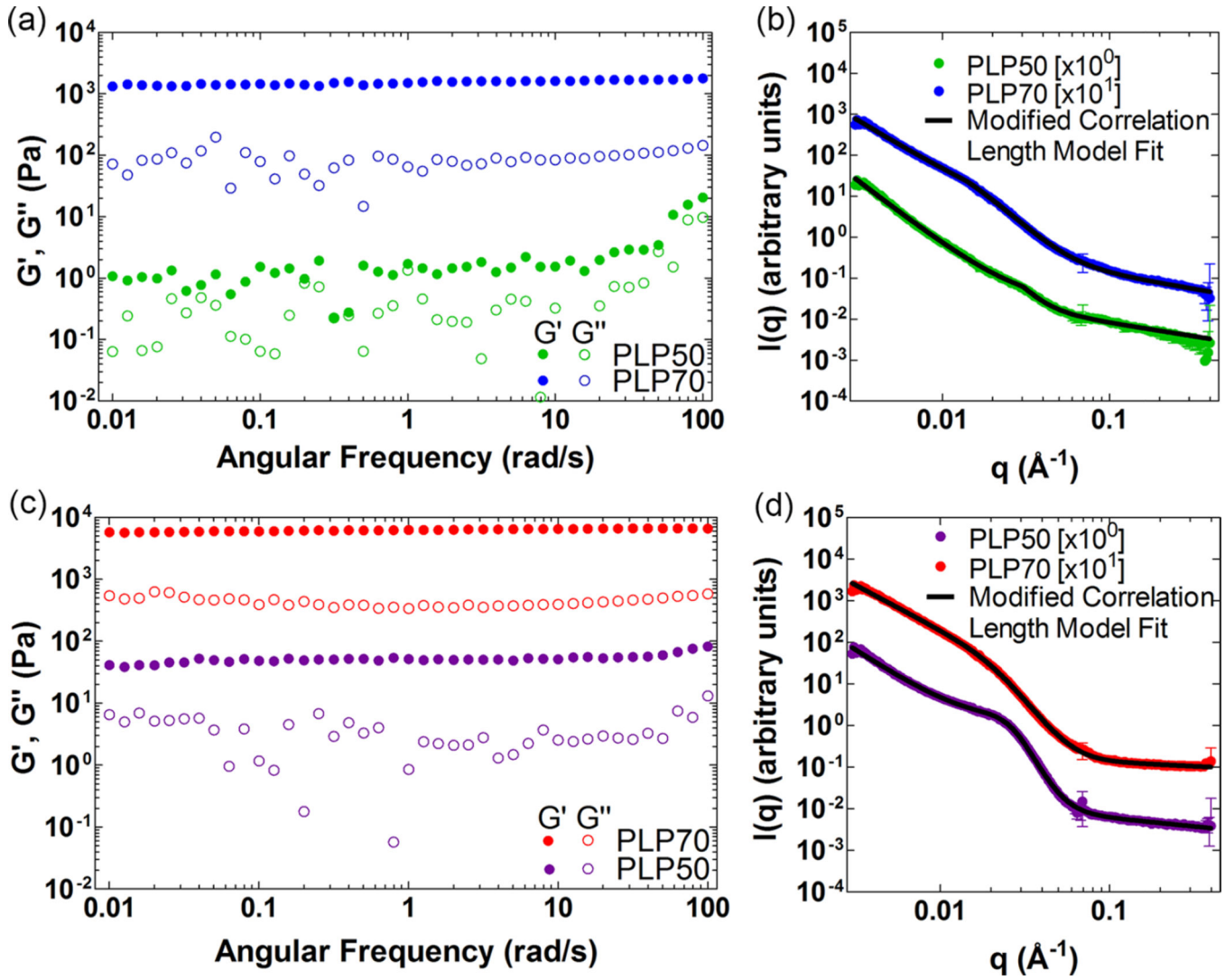

Figure 5.

Frequency sweeps of aqueous 10 wt % PLP70 and PLP50 (a) at 5 °C and (b) the corresponding SANS curves for the samples. Frequency sweeps were also performed for 10 wt % PLP70 and PLP50 at (c) 35 °C, with accompanying (d) SANS plots for the same samples. Gels were equilibrated at each temperature for 1 h prior to measurements. SANS curves are offset for clarity.

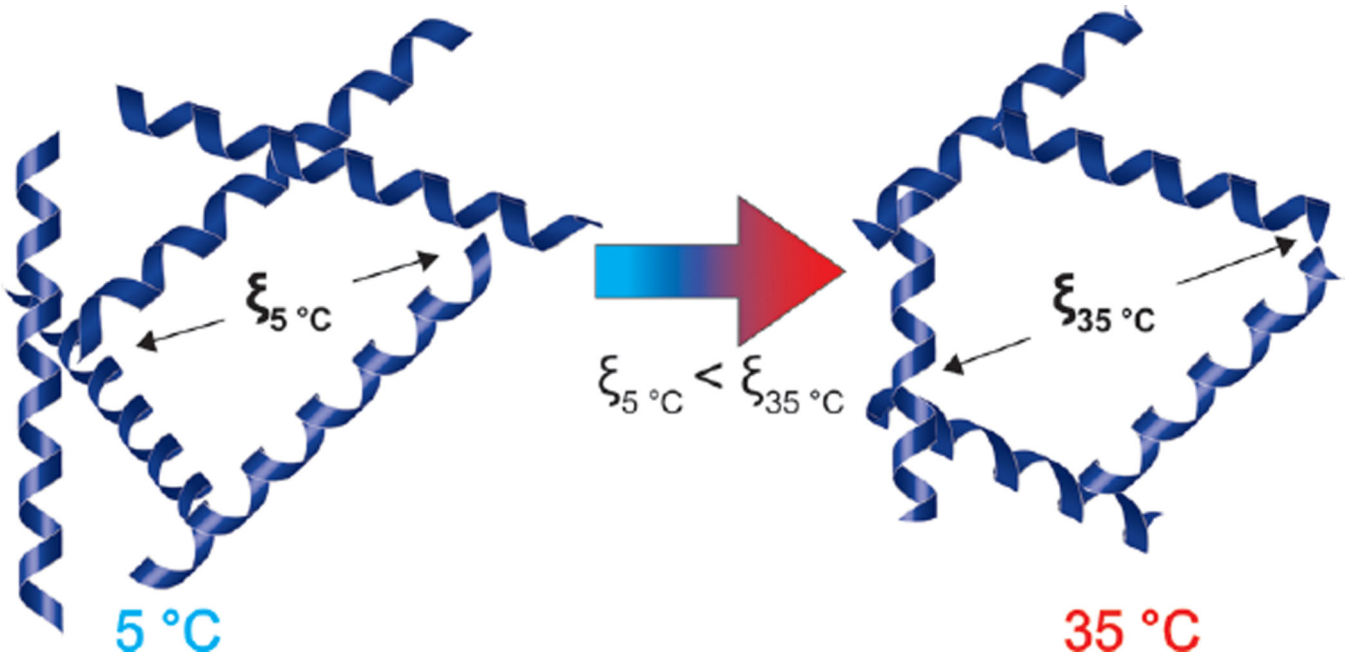

Figure 6.
Proposed cartoon representation of changing PLP gel structure during a temperature increase.

Table 1

Molecular Characterization of Synthesized PLP Homopolymers

Sample	$M_n \times 10^{3a}$ (g/mol)	$M_n \times 10^{3b}$ (g/mol)	M_w/M_n	N_{PLP}	L_{PLP} [c] (nm)
PLP40	3.9 ± 0.1	4.3 ± 0.3	1.29	40	12.4
PLP50	4.9 ± 0.2	5.7 ± 0.3	1.30	50	15.5
PLP70	6.8 ± 0.2	8.2 ± 0.4	1.28	70	21.7

[a] Molecular weight of PLP from ^{1}H NMR in CF_3COOD; $MW_{LP\text{-}monomer}$ = 97 g/mol.

[b] Molecular weight determined by GPC in 0.1 M $NaNO_3$ solution of water/acetonitrile 80/20.

[c] Calculated length for ideal PLP II helices using 3.1 Å/residue. Due to heating and possible intermediate structures,[24c] the actual dimensions are expected to be lower.

Table 2

Modified Correlation Length Model Fits for Porod Exponent and Correlation Length

Sample	*T* °C	Porod	ξ (nm)
PLP70 at 1 wt %	5	2.3 ± 0.08	$4.4 \pm 9 \times 10^{-03}$
PLP70 at 10 wt %	5	2.5 ± 0.03	$5.0 \pm 1 \times 10^{-02}$
PLP70 at 15 wt %	5	2.5 ± 0.03	$5.5 \pm 8 \times 10^{-02}$
PLP70 at 1 wt %	35	2.2 ± 0.07	$4.7 \pm 7 \times 10^{-03}$
PLP70 at 10 wt %	35	2.2 ± 0.02	$6.7 \pm 5 \times 10^{-02}$
PLP70 at 15 wt %	35	2.2 ± 0.03	$7.2 \pm 8 \times 10^{-02}$
PLP50 at 10 wt %	5	3.2 ± 0.06	$5.5 \pm 4 \times 10^{-01}$
PLP50 at 10 wt %	35	2.7 ± 0.05	$10.2 \pm 5 \times 10^{-03}$